

Isomeric and hybrid isomeric-vibrational states of Wigner molecules

S. A. Blundell* and S. Chacko†

SPSMS, UMR-E 9001, CEA-INAC/UJF-Grenoble 1, 17 rue des Martyrs, 38054 Grenoble cedex 9, France

(Received 8 February 2010; published 25 March 2010)

An accurate configuration-interaction method employing a numerical mean-field basis set is used to study the excitation spectrum of Wigner molecules, including isomeric excitations, in small parabolic quantum dots. We find that at intermediate electron densities ($r_s \sim 8a_0^* - 20a_0^*$), in the regime of strong interaction and partial Wigner localization, there are inversions of the usual Born-Oppenheimer ordering of isomeric and vibrational excitations, yielding low-lying isomeric excitations. Quantum-mechanical hybridization of different isomers can occur near an avoided crossing of a vibrational and an isomeric excitation. These findings suggest the possibility of observing isomers and hybrid isomeric-vibrational states experimentally.

DOI: 10.1103/PhysRevB.81.121104

PACS number(s): 73.21.La, 73.22.Gk

Semiconductor quantum dots (QDs), or *artificial atoms*, are formed when a finite number (tens or hundreds) of free-carrier electrons (or holes) are confined electrostatically to nanometer-sized regions.¹ Unlike real atoms or molecules, or other finite-fermion systems such as nuclei or metallic clusters, which have sizes fixed by the physics of their constituents, the size, shape, and average electronic density of a QD may be varied experimentally.¹ One can therefore study the low-density regime of strong interaction, where the electronic interaction energy greatly exceeds the kinetic energy and the electrons are expected to localize into a “Wigner molecule,”^{2,3} a finite-size analog of the transition to a crystal lattice (Wigner solid) in the low-density infinite homogeneous electron gas.⁴ Experimentally, it has been possible to observe evidence of the bulk transition to a Wigner solid⁵ but the effect in finite-sized systems has proved more elusive. Recent experimental work on excited states of four-electron QDs at high density has, however, revealed “rigid-rotor” behavior of a molecular-like state.⁶ With further advances in semiconductor QD growth techniques, it may soon be possible to observe Wigner localization in quasi-two-dimensional (2D) QDs at zero magnetic field.

There has been much recent theoretical work devoted to Wigner localization in QDs.^{6–10} Very precise studies of quasi-2D Wigner-molecule ground states have recently become possible using quantum Monte Carlo (QMC) in the variational Monte Carlo/diffusion Monte Carlo (VMC/DMC) form,⁸ which has been applied for up to $N=18$ electrons and to low densities $r_s \leq 55a_0^*$.^{8,10} [Here $r_s = (\pi\bar{n})^{-1/2}$ for a quasi-2D dot, where \bar{n} is the average electron density in the plane. We use effective atomic units¹ throughout, with a_0^* the effective Bohr radius in the semiconductor and Ha^* the effective hartree.] A drawback of the VMC/DMC approach, however, is that it is unsuitable for studying the excited states of the system (aside from the lowest-energy state of a given symmetry).⁸ A quantum many-body approach that *can* apply, in principle, to excited states is configuration interaction (CI) (Refs. 7 and 11) but this method has so far been possible only for more limited r_s (e.g., $r_s \leq 20a_0^*$ in Ref. 6) and size (e.g., $N \leq 8$ in Ref. 7), and it also has significantly worse reported precision than VMC/DMC.

In this work, we use a CI approach employing a numerical mean-field basis, which we have developed recently. This method yields vastly improved convergence in the Wigner-

molecule regime compared to CI with the more commonly used harmonic-oscillator orbitals^{7,11} because the low-lying members of the mean-field basis set already “know” about the localization. As we shall see, the method gives energies that are competitive with (or better than) VMC/DMC in precision for $N=6$; it is also stable up to much higher $r_s \sim 50a_0^*$ than earlier CI treatments. These properties, together with the capability of CI of extracting excited states, allow us to study systematically the isomeric-vibrational states of the Wigner molecule down to low densities. While several earlier theoretical studies at low densities have focused on rotational and vibrational excited states of small systems with up to $N=5$ electrons (e.g., Refs. 12 and 13), to our knowledge, there has been no quantum many-body study of the isomeric excited states and their interplay with vibrational modes in this density regime. Yet parabolic QDs with $N \geq 6$ electrons, in general, have more than one classical isomer¹⁴ (that is, stable arrangements of classical point electrons in a parabolic trap) so that isomeric states should be a basic feature of the spectrum of a Wigner molecule for all but the smallest systems ($N \leq 5$). We show here that at the intermediate densities that may be reached in initial experiments (e.g., $r_s \sim 8a_0^* - 20a_0^*$), isomeric states are in fact likely to be the *first* excited level for a given orbital angular momentum L_z , reversing the more natural Born-Oppenheimer (BO)-type ordering of energy levels that would favor a low-lying vibrational excited mode. This finding suggests that it may be possible to observe isomeric states experimentally. Note also that molecular-like states may be induced at high densities ($r_s \approx 1.5a_0^*$) by an intense magnetic field or by very high orbital angular momentum.¹⁵

As an example of our CI method, Table I shows the energy of the ground state of an $N=6$ electron parabolic QD for a density parameter $\lambda=8$ (corresponding to $r_s \approx 12a_0^*$), where $\lambda = l_0/a_0^*$ is the ratio of the parabolic confinement length $l_0 = \sqrt{\hbar/m^*\omega_0}$ to the effective Bohr radius. We here assume a quasi-2D electron system in the effective-mass approximation,¹ confined by a circular parabolic potential $V_{\text{ext}}(r) = m^*\omega_0^2 r^2/2$. We have organized the full CI calculation by degree of excitation from a “model space,” which consists of all determinants that may be formed from the lowest 8 or 10 states in the single-particle basis. The model space in lowest order is already sufficient to give a semiquantitative description of the many-body state. An extrapolation to the

TABLE I. CI energies of the ground state ($S=0$) of the $N=6$ electron parabolic dot for density parameter $\lambda=8(r_s \approx 12a_0^*)$, using a model space formed from either 10 [$\nu 10$] or 8 [$\nu 8$] single-particle states. Units: Ha^* .

Excitation	[$\nu 10$]	[$\nu 8$]
Lowest order	0.96757	0.97614
Singles	-0.01691(6)	-0.01988(5)
Doubles	-0.00672(1)	-0.01023(2)
Triples	-0.00153(1)	-0.00309(1)
Quadruples	-0.00027(2)	-0.00073(1)
Pentuples	-0.00003(1)	-0.00008(2)
Hexuples	0.00000	-0.00001
Total	0.94211(6)	0.94213(6)
QMC, Ref. 8	0.942580(5)	

basis-set limit is also made (where the upper energy cutoff of the basis set is allowed to go to infinity), yielding the estimated error shown; this error is the only error in a full CI calculation.

Our CI energy is about $0.46(6) \text{ mHa}^*$ lower than that from VMC/DMC.⁸ We consistently converge to our value for the ground-state energy not only for the different sizes of model space shown but also for different basis sets corresponding to different mean fields. Since our energy is lower (more negative) than the VMC/DMC energy, which may be regarded as a variational upper bound with a known statistical error,⁸ a possible explanation for the discrepancy is that we have revealed the *systematic* error in the VMC/DMC energy arising from the fixed-node approximation.⁸ This pattern is repeated for some of the other energies reported in Ref. 8; the full details of our calculation method and these other comparisons will be given elsewhere.

The main features of the excitation spectrum are exhibited by the $N=6$ electron dot, which is the smallest system to show spin, rotational, vibrational, and isomeric excitations. For six electrons, the classically stable configurations (see Fig. 1) consist of a pentagonal (1, 5) ground-state isomer and a staggered hexagonal (0, 6) excited isomer¹⁴ (the perfect hexagon being a saddle point on the potential-energy surface). Now, the average Wigner-Seitz radius r_s is given approximately by $r_s^3 = 1/(\omega_0^2 \sqrt{N})$ (in effective atomic units).¹⁶ Taking this as the definition of r_s and using the data for the classical system (from Ref. 14 and our own calculations), we infer the following estimates of excitation energies: $\Delta E_{\text{iso}} = 0.0714r_s^{-1}$, $\Delta E_{\text{vib}} = 0.415r_s^{-3/2}$, and $\Delta E_{\text{rot}} = 0.0309r_s^{-2}$ (in units of Ha^* with r_s in a_0^*). Here ΔE_{iso} is the energy difference between the two classical isomers (Fig. 1), ΔE_{vib} is the energy of one vibrational quantum in the lowest-frequency normal mode of the ground-state (1,5) isomer, and ΔE_{rot} is the S -to- P -wave rotational excitation energy of this isomer. Owing to the differing dependencies on the length scale r_s , for sufficiently large r_s , we must eventually find $\Delta E_{\text{iso}} \gg \Delta E_{\text{vib}} \gg \Delta E_{\text{rot}}$, that is, a BO-type separation of energy scales.

To gain some idea of the appropriate length scales for the six-electron dot, we have plotted these approximate excita-

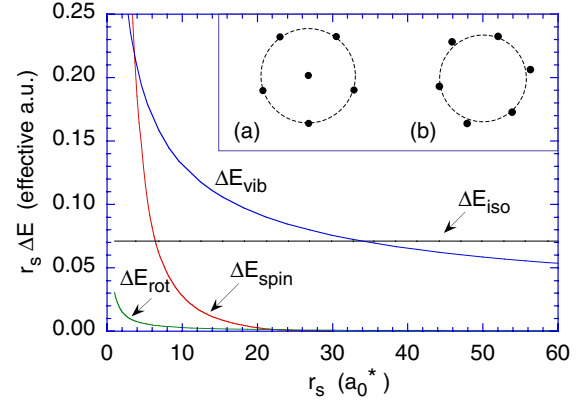


FIG. 1. (Color online) Approximate excitation energies of the six-electron parabolic dot versus Wigner-Seitz radius r_s (see text). Energies are scaled by r_s . Inset: stable configurations of the classical six-electron parabolic dot (from Ref. 14): (a) pentagonal ground-state configuration and (b) excited isomer (staggered hexagon).

tion energies (scaled by r_s) in Fig. 1. The figure shows that the strict BO ordering of energies will be realized only for $r_s \gg 34a_0^*$. At $r_s \approx 34a_0^*$, there is a crossover between ΔE_{vib} and ΔE_{iso} , and at smaller r_s , there is then an inversion of the usual BO ordering, with the isomeric excitation energy comparable to or smaller than the vibrational excitation energies.

On the other hand, for all $r_s \geq 2a_0^*$, the rotational excitation energy is small, $\Delta E_{\text{rot}} \ll \Delta E_{\text{vib}}$, ΔE_{iso} , and so we may expect the rotational motion to decouple well for this entire range of r_s (at least, for low to moderate L_z). This observation is consistent with the experimental evidence found by Kalliakos *et al.*⁶ for rigid-rotor behavior of low-angular-momentum states in $N=4$ electron dots already for $r_s \approx 2a_0^*$.

We have also shown in Fig. 1 a typical spin excitation energy ΔE_{spin} , which is defined as the energy splitting of the $S=3$ excited state and the $S=0$ ground state in the ground-state spin multiplet. According to our CI calculations, this is well fit by $\Delta E_{\text{spin}} = 0.056 \exp(-0.29r_s) \text{ Ha}^*$ for $6a_0^* < r_s < 30a_0^*$ (see also the QMC data in Refs. 8 and 17). For $r_s \leq 6a_0^*$, the spin energies (exchange interactions) and the isomeric and vibrational excitation energies are all nominally comparable.

We now turn to an analysis of the excited states using our quantum many-body CI procedure. Since we are here primarily interested in the isomeric and vibrational degrees of freedom, we shall consider only S -wave ($L_z=0$) excited states. Now, because the exact density is circularly symmetric (in the “laboratory” frame),¹⁸ we analyze the underlying pattern of Wigner localization by means of (spin-summed) pair-correlation functions (PCFs),^{11,13,15} $g(\mathbf{r}_0, \mathbf{r}) = \langle \sum_{i \neq j} \delta(\mathbf{r}_0 - \mathbf{r}_i) \delta(\mathbf{r} - \mathbf{r}_j) \rangle$. The quantity $g(\mathbf{r}_0, \mathbf{r})$ is proportional to the conditional probability of finding an electron at \mathbf{r} given that a second, reference electron is located at \mathbf{r}_0 . In Fig. 2, we plot PCFs for the six-electron QD as a function of \mathbf{r} , with the position \mathbf{r}_0 of the reference electron indicated by a dot. The PCFs here have been converged to better than a few percent and display a pronounced “correlation hole”⁸ at $\mathbf{r} = \mathbf{r}_0$.

For $r_s = 20a_0^* - 50a_0^*$, the spin excitation energies are very small (see Fig. 1), and the excited states for given L_z thus

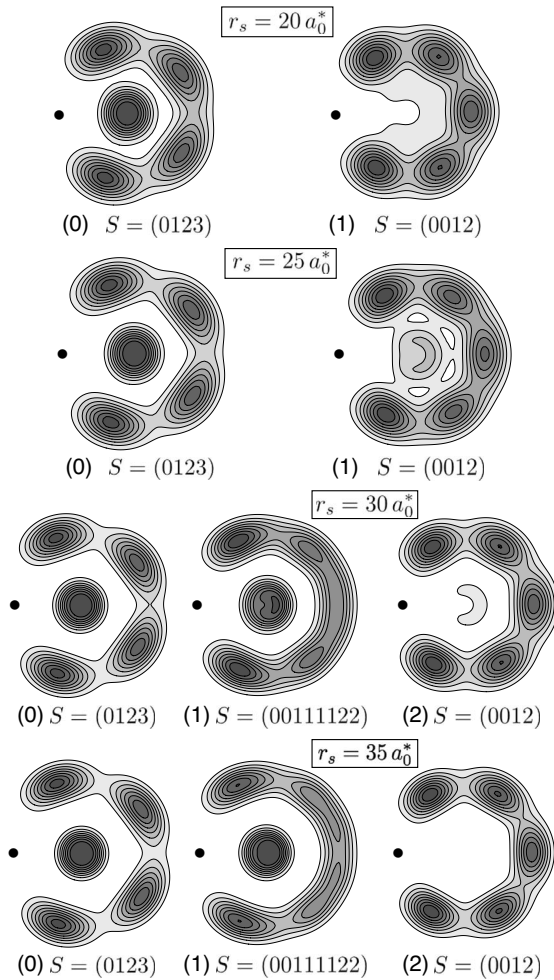


FIG. 2. Representative pair-correlation functions of S -wave spin multiplets of the six-electron parabolic dot for $r_s = 20a_0^* - 35a_0^*$. (0), (1), ..., etc., signify the ground-state spin multiplet, the first excited multiplet, ..., etc., respectively. The fixed reference electron is indicated by a dot and the set of total spins present in each multiplet is also given.

consist of a series of nearly degenerate spin multiplets; these multiplets are typically separated from each other by a few mHa^* due to the isomeric and vibrational degrees of freedom. The PCFs for each member of a spin multiplet are found to be very nearly the same (in this range of r_s) so in Fig. 2 we show only a representative PCF for each multiplet. For all $r_s = 20a_0^* - 50a_0^*$, the ground-state geometry corresponds to the classical pentagonal (1,5) ground-state structure.¹⁰ The ground-state spin multiplet has a multiplicity of 4 (number of S values present in the multiplet) with allowed total spin quantum numbers $S=0, 1, 2, \text{ and } 3$.

Now, at $r_s = 20a_0^*$, we see from Fig. 2 that the first excited multiplet corresponds to a quite pure hexagonal (0,6) isomer. Thus, we confirm that there is indeed an inversion of the usual BO ordering of isomeric and vibrational energies at this r_s , consistent with the simple classical argument (Fig. 1). Interestingly, the allowed spins $S=(0,0,1,2)$ and multiplicity of 4 for this isomer are those associated with the perfect C_{6v} hexagonal symmetry,¹⁹ and not with the staggered hexagonal geometry of the classical isomer [Fig. 1(b)], which

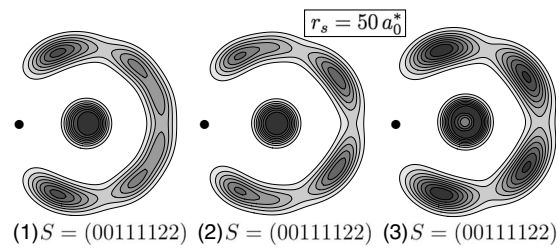


FIG. 3. Representative pair-correlation functions of the (1) first, (2) second, and (3) third excited S -wave spin multiplets for the six-electron dot at $r_s = 50a_0^*$. See Fig. 2 for further conventions.

may be shown to lead to a different set of allowed spins. (A detailed analysis of the group theoretical considerations for all states in this Rapid Communication will be presented elsewhere.)

At $r_s = 35a_0^*$, however, we find that another multiplet has come down to lie between the (1,5) ground-state and the (0,6) excited isomer. This corresponds to one vibrational quantum in the (1,5) geometry. Again, the allowed spins $S=(0,0,1,1,1,1,2,2)$ and multiplicity of 8 are just those expected from a group-theory analysis,¹⁹ confirming this interpretation. We see from Fig. 2 that the crossover between the isomeric and the vibrational excitation here occurs between $r_s = 25a_0^*$ and $30a_0^*$, quite close to the value $r_s \approx 34a_0^*$, we predicted from the simple classical argument. Interestingly, near the (avoided) crossing, the excited states mix and show evidence of quantum-mechanical hybridization between (1,5) and (0,6) isomers. Thus, the (0,6) structures show a central peak while the (1,5) vibrational mode at $r_s = 30a_0^*$ shows a very weakly formed sixth peak in the outer ring.

Moving on to $r_s = 50a_0^*$, we find that *three* vibrational multiplets have come down to lie between the ground (1,5) and the excited (0,6) isomer; they are shown in Fig. 3. This confirms the trend that vibrational excitation energies decrease faster with r_s than the isomeric excitation energy so that the system is beginning to come into a more typical BO energy ordering with $\Delta E_{\text{vib}} \leq \Delta E_{\text{iso}}$. The pattern of allowed spins can be shown to imply that these multiplets correspond to one vibrational quantum in three different normal modes. Note that the central peak in the third excited state shows clear evidence of a vibrational excitation.

There is a different type of isomeric hybridization around $r_s \approx 6a_0^*$. At $r_s = 4a_0^*$, the ground state ($S=0$) shows partial Wigner localization in a predominantly (0,6) [and not (1,5)] geometry¹¹ but as r_s increases, the ground state transforms gradually into a (1,5) geometry,¹⁰ the transformation being quite complete by $r_s \approx 10a_0^*$. In more detail, we find that at $r_s = 4a_0^*$, the first spin-0 S -wave *excited* state has a predominantly (1,5) and (0,6) isomers; thus, the classical energy ordering of (1,5) and (0,6) isomers is for this r_s (and $S=0$) inverted. As r_s increases, there is isomeric hybridization and a gradual interchange of (1,5) and (0,6) geometries. By $r_s = 10a_0^*$, the two isomers are quite pure and in their classical energy ordering with (1,5) below (0,6), and they stay this way for all higher r_s (see Figs. 2 and 3). The inversion of the (1,5) and (0,6) energy ordering for $r_s = 4a_0^*$ is presumably an effect of mixing of isomeric states by the exchange interactions (or other atomiclike correlation effects); as the spin energy de-

creases relative to the isomeric excitation energy (see Fig. 1), the two isomers eventually regain their classical energy ordering.

One can generalize these results to higher N using classical estimates of excitation energies (similar to Fig. 1). Thus, one finds that rotational excitation energies are generally small, $\Delta E_{\text{rot}} \ll \Delta E_{\text{vib}}, \Delta E_{\text{iso}}$. Furthermore, the excitation energies ΔE_{vib} of the majority²⁰ of normal modes are greater than those of the first isomer ΔE_{iso} at intermediate $r_s \sim 20a_0^*$ (at least up to $N=20$, which we have studied explicitly). Thus, for these larger dots also, the first excited level (spin multiplet) for fixed L_z at intermediate r_s can be an isomer rather than a vibrational mode of the ground state. For instance, for $N=19$, the classical ground state has a (1,6,12) geometry and there is a (1,7,11) excited isomer;¹⁴ the crossover condition $\Delta E_{\text{vib}} = \Delta E_{\text{iso}}$ here occurs at $r_s \approx 800a_0^*$ so that the strict BO

energy ordering of isomeric and vibrational excitations would be expected to occur only for $r_s \gg 800a_0^*$.

The fact that isomeric states are expected to be low-lying excitations at intermediate densities may facilitate their observation. Possible experimental signatures include (i) selection rules for optical processes such as inelastic scattering⁶ or absorption, which depend on the symmetry of the isomer or vibrational normal mode and are directly analogous to those for molecules;¹⁹ (ii) Franck-Condon-type factors¹⁹ for inter-isomer transition rates; and (iii) the pattern of allowed spins and multiplicities (e.g., Figs. 2 and 3), which depends on the isomer or vibrational mode and may be inferable from spin selection rules. In addition, recent improvements in high-spatial-resolution scanning probe techniques²¹ may make it possible to map out the spatial distribution of a Wigner molecule, leading to a direct observation of the geometry.

*steven.blundell@cea.fr

†Present address: Centre for Computational Biology and Bioinformatics, Jawaharlal Nehru University, New Delhi 110 067, India; sajeev.chacko@gmail.com

¹L. Jacak, P. Hawrylak, and A. Wójs, *Quantum Dots* (Springer, Berlin, 1998).

²R. Egger, W. Häusler, C. H. Mak, and H. Grabert, *Phys. Rev. Lett.* **82**, 3320 (1999).

³C. Yannouleas and U. Landman, *Phys. Rev. Lett.* **82**, 5325 (1999).

⁴E. Wigner, *Phys. Rev.* **46**, 1002 (1934).

⁵V. M. Pudalov, M. D'Iorio, S. V. Kravchenko, and J. W. Campbell, *Phys. Rev. Lett.* **70**, 1866 (1993).

⁶S. Kalliakos, M. Rontani, V. Pellegrini, C. P. García, A. Pinczuk, G. Goldoni, E. Molinari, L. N. Pfeiffer, and K. W. West, *Nat. Phys.* **4**, 467 (2008).

⁷M. Rontani, C. Cavazzoni, D. Bellucci, and G. Goldoni, *J. Chem. Phys.* **124**, 124102 (2006).

⁸A. Ghosal, A. D. Güçlü, C. J. Umrigar, D. Ullmo, and H. U. Baranger, *Nat. Phys.* **2**, 336 (2006); *Phys. Rev. B* **76**, 085341 (2007).

⁹C. Yannouleas and U. Landman, *Rep. Prog. Phys.* **70**, 2067 (2007).

¹⁰A. D. Güçlü, A. Ghosal, C. J. Umrigar, and H. U. Baranger, *Phys. Rev. B* **77**, 041301(R) (2008).

¹¹S. M. Reimann, M. Koskinen, and M. Manninen, *Phys. Rev. B*

62, 8108 (2000).

¹²W. Häusler, *Europhys. Lett.* **49**, 231 (2000).

¹³C. Yannouleas and U. Landman, *Phys. Rev. Lett.* **85**, 1726 (2000).

¹⁴F. Bolton and U. Rössler, *Superlattices Microstruct.* **13**, 139 (1993); V. M. Bedanov and F. M. Peeters, *Phys. Rev. B* **49**, 2667 (1994).

¹⁵P. A. Maksym, *Phys. Rev. B* **53**, 10871 (1996); M. Manninen, S. Viefers, M. Koskinen, and S. M. Reimann, *ibid.* **64**, 245322 (2001); J.-P. Nikkarila and M. Manninen, *Phys. Rev. A* **76**, 013622 (2007).

¹⁶M. Koskinen, M. Manninen, and S. M. Reimann, *Phys. Rev. Lett.* **79**, 1389 (1997).

¹⁷L. Zeng, W. Geist, W. Y. Ruan, C. J. Umrigar, and M. Y. Chou, *Phys. Rev. B* **79**, 235334 (2009).

¹⁸K. Hirose and N. S. Wingreen, *Phys. Rev. B* **59**, 4604 (1999).

¹⁹J. M. Hollas, *Symmetry in Molecules* (Chapman and Hall, London, 1972); G. Herzberg, *Molecular Spectra and Molecular Structure* (Van Nostrand, Princeton, 1967), Vol. 3.

²⁰The main possible exceptions are normal modes in which the concentric rings of electrons rotate with respect to one another, which (classically) sometimes have low frequency with $\Delta E_{\text{vib}} < \Delta E_{\text{iso}}$ at $r_s = 20a_0^*$.

²¹See, for example, A. M. Mintairov, Y. Chu, Y. He, S. Blokhin, A. Nadtochy, M. Maximov, V. Tokranov, S. Oktyabrsky, and J. L. Merz, *Phys. Rev. B* **77**, 195322 (2008), and references therein.